



## Raman spectroscopy of racemic ibuprofen: Evidence of molecular disorder in phase II

Alain Hédoux<sup>a,\*</sup>, Yannick Guinet<sup>a</sup>, Patrick Derollez<sup>a</sup>, Emeline Dudognon<sup>a</sup>, Natalia T. Correia<sup>a,b</sup>

<sup>a</sup> Univ Lille Nord de France, F-59000 Lille, France USTL, UMR 8207, F-59650 Villeneuve d'Ascq, France

<sup>b</sup> REQUIMTE, Departamento de Química, Faculdade de Ciências e Tecnologia da Universidade Nova de Lisboa, 2829-516 Caparica, Portugal

### ARTICLE INFO

#### Article history:

Received 2 June 2011

Received in revised form

13 September 2011

Accepted 15 September 2011

Available online 21 September 2011

#### Keywords:

Disordered crystalline phase

Low-frequency Raman spectroscopy

Phase transformation

Ibuprofen

Molecular glass-forming systems

### ABSTRACT

Low- and high-frequency Raman experiments in the 5–200 cm<sup>-1</sup> and 600–1800 cm<sup>-1</sup> ranges were carried out in the crystalline and amorphous states of ibuprofen. Low-frequency investigations indubitably reveal the existence of a molecular disorder in the metastable phase (phase II), through the observation of quasielastic contribution below 30 cm<sup>-1</sup>, and the absence of phonon peaks in the Raman susceptibility which mimics the density of vibrational states of an amorphous state. High-frequency Raman spectra indicate a local order in phase II similar to that in the glassy state. Both dynamic and static molecular disorder could contribute to the Raman signatures of the disorder in crystalline phase II. Raman investigations suggest that phase II can be considered as a transient metastable state in the devitrification process of ibuprofen upon heating from a far from equilibrium state toward the stable phase I.

© 2011 Elsevier B.V. All rights reserved.

### 1. Introduction

The detailed knowledge on the polymorphism of pharmaceuticals has important consequences for the production of drugs. First, polymorphic varieties can have different physical properties, e.g. different solubilities, that can lead to drastically different bio-availabilities of two forms. Second, during the processing (milling, spray drying, lyophilization, tablet compaction, etc.) and the storage of pharmaceutical compounds, various degrees of disorder in the form of crystal defects can be generated. Disordered materials are inherently metastable and will tend to convert into a more thermodynamically stable crystalline form. In this context, investigating the degree of disorder or thermodynamic stability of pharmaceutical materials is crucial in their formulation, storage and processing. Ibuprofen, 2(4-isobutylphenyl) propanoic acid, is a frequently used non-steroidal anti-inflammatory drug. It is currently available as a racemic compound of S(+)-ibuprofen and R(–)-ibuprofen, the (S+) conformation corresponding to the pharmacologically active form (Adams et al., 1976). Despite the evidence of different crystal morphologies (Lee et al., 2006; Nada et al., 2005; Rasenack and Muller, 2002a,b), only one crystalline phase

(phase I) was identified until the recent detection of a metastable phase (phase II) from X-ray diffraction and differential scanning calorimetry investigations (Dudognon et al., 2008). The metastable state was formed after rapid quench of the melt at 143 K, i.e. well below the glass transition temperature ( $T_g \approx 228$  K, Johari et al., 2007), isothermal annealing during 1 h and heated at 258 K. At this temperature, undercooled liquid isothermally transforms toward the new metastable phase II. Structural determinations of the metastable (Derollez et al., 2010) and stable (Connell, 1974; Shankland et al., 1997) phases lead to similar molecular organizations in cyclic dimers via hydrogen bonding in a monoclinic unit cell with the same space group ( $P2_1/c$ ). The structural organization of ibuprofen molecules in phases I and II are plotted in Fig. 1. The main difference between the two structural descriptions results in the orientation of hydrogen bonding between two enantiomers, perpendicular to dimer chains linking the different chains in the stable phase I, and in the direction of dimer chains in phase II. These two different kinds of molecular association can explain the stronger cohesion between dimer chains in phase I, and hence a cell volume in phase II 5% larger than that in phase I at the same temperature (258 K). It was reported that, given the abnormally high value obtained for the overall Debye–Waller factor, it was kept fixed during structural refinements of phase II (Derollez et al., 2010). It can be also found in the structure determination a significant difference between reliability factors obtained for the (Le Bail) profile fitting of the diffraction pattern (~8%) and for the Rietveld refinements (~14%) including the fit of Bragg peak intensities associated

\* Corresponding author at: Univ-Lille 1, UMET-Bât. P5, Bd Paul Langevin, Cité Scientifique, 59665 Villeneuve d'Ascq Cedex, France. Tel.: +33 320434677; fax: +33 320436857.

E-mail address: [alain.hedoux@univ-lille1.fr](mailto:alain.hedoux@univ-lille1.fr) (A. Hédoux).

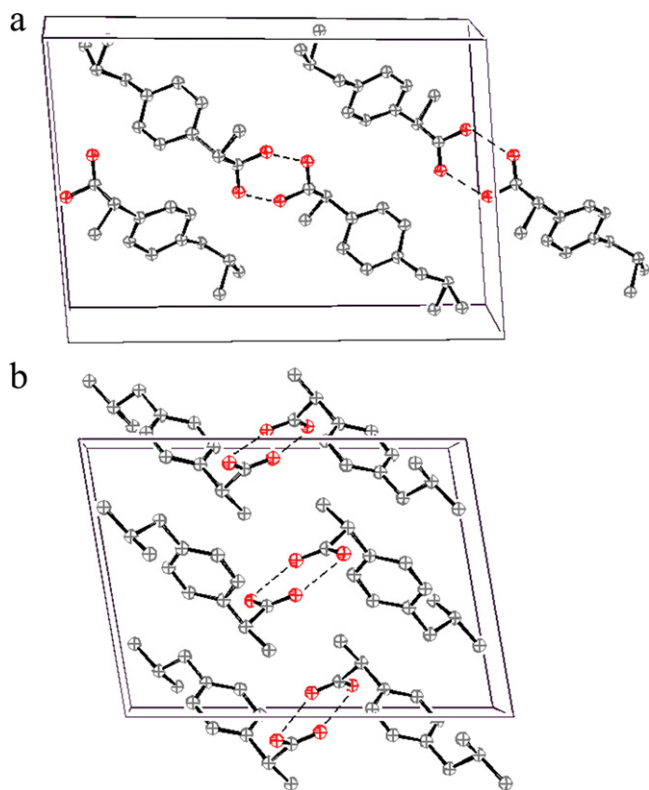


**Fig. 1.** Representation in the (a and b) plane of the molecular organization and the unit cell of ibuprofen. (a) In phase II, from Derollez et al. (2010). (b) In phase I, from Shankland et al. (1997).

to the atomic positions. These abnormal features in the structural refinement of phase II suggest the existence of a positional atomic disorder not considered in the refinement of the structural model. The analysis of the dynamics of the different states of ibuprofen is needed to give a better structural description and a better insight into stability conditions of phase II. It was shown that low-frequency Raman spectroscopy can clarify structural description in different molecular disordered systems (Hédoux et al., 2011a, 2004, 2006). Consequently, Raman investigations were carried out in the different states of racemic ibuprofen.

## 2. Materials and methods

### 2.1. Materials

Racemic ibuprofen, 2(4-isobutylphenyl) propanoic acid, was purchased from Sigma Chemical Company (lot No. 026H1368), with a purity of 99.8% and used without further purification.

### 2.2. Raman spectroscopy

#### 2.2.1. Experimental procedure

Raman spectra were recorded in the 5–200  $\text{cm}^{-1}$  range, in VV+VH geometry to obtain non polarized light-scattering spectrum under a scattering angle  $\theta = 180^\circ$ , using the 514.5 nm line of a mixed argon–krypton Coherent laser. The spectrometer is composed of a double monochromator comprising four mirrors characterized by a focal length of 800 mm, and a spectrograph. The entrance and exit slits are opened and kept to 200  $\mu\text{m}$ , determining for the incident radiation a resolution of nearly 2  $\text{cm}^{-1}$  in the low-frequency range. It is the monochromator which prohibits the exciting line from entering the spectrograph field. The well-adapted positioning of the monochromator with respect to

the spectrograph and the choice of experimental conditions (incident radiation, slit width) allow a rejection of exciting light down to 5  $\text{cm}^{-1}$ . The spectrometer is equipped with a liquid nitrogen cooled charge coupled device detector. Temperature control of the sample was provided by an Oxford nitrogen-flux device which keeps temperature fluctuation within 0.1 K. Two series of experiments were performed. (i) The first set of experiments was carried out on a small volume of sample ( $\sim 0.002 \text{ cm}^3$ ) placed into a Lindemann glass capillary ( $\varnothing = 0.7 \text{ mm}$ ). In this case a thermal history rigorously similar to that used to analyze phase II by X-ray diffraction (Derollez et al., 2010; Dudognon et al., 2008) was imposed to the sample, i.e. the powder was melt at 373 K and cooled down to 143 K at 6 K/min where the sample was annealed for 1 h. Some cracks were clearly observed below 160 K, via the deviation of the laser beam through the cylindrical container and a turbidity of the under-cooled liquid. The sample was then heated at 260 K for analyzing the isothermal transformation of the under-cooled liquid toward phase II. The small volume of sample analyzed requires an acquisition time of 10 min. (ii) In the second set of experiments, a greater amount of Ibuprofen powder ( $\sim 0.4 \text{ cm}^3$ ) was loaded in a hermetically sealed spherical pyrex cell. The large analyzed scattering volume ( $\sim 0.4 \text{ cm}^3$ ) provides Raman spectra of high quality compared to the set of experiments (i), and allows us to record low-frequency Raman spectra in the 5–200  $\text{cm}^{-1}$  range in 2 min. In this case, the sample was quenched from 360 K down to 190 K, i.e. more than 40 K below  $T_g$  by shifting the sample located in hot air stream (360 K) into the regulated nitrogen flux (190 K) of the Oxford device. Some cracks were observed at higher temperature ( $\sim 190 \text{ K}$ ) than in the first set of experiments. The temperature is then increased (6 K/min) from 190 K up to 260 K (32 K above the glass transition temperature), for isothermal annealing. The isothermal transformation of the under-cooled liquid was investigated from the analysis of the temporal dependence of the low-frequency spectrum. Raman investigations have been also carried out in the 600–1800  $\text{cm}^{-1}$  spectrum where intra-molecular vibrations can be detected and used to analyze the local order.

#### 2.2.2. Analysis of Raman spectra of molecular compounds

Raman spectroscopy gives the original opportunity to analyze the three kinds of molecular motions existing in the organic molecular compounds, in the framework of the rigid body model. (i) The internal motions, corresponding to vibrations within the molecule, (ii) the semi-internal (or semi-external) motions usually corresponding to very large amplitude rotations of a group of atoms within the molecule or the whole of the molecule, and (iii) the external motions associated to intermolecular and collective vibrations, named lattice vibrations or phonons in the crystalline state, and consisting in a vibrational density of states in the solid amorphous state. The pronounced contrast between strong covalent intramolecular interactions and soft van der Waals intermolecular attractions or hydrogen bonding association is reflected in the Raman spectra by a spectral gap between external and internal peaks. However, in disordered molecular systems the low-frequency Raman intensity results from the overlapping contributions of semi-external motions, associated with the quasi-elastic (QES) intensity, and external or collective motions (Hédoux et al., 2006, 2011b). Internal modes are sensitive to the local molecular organization. A broadening of Raman bands generally reflects the existence of different molecular configurations or orientations at equivalent sites in a crystal (Denicourt et al., 2003). On the other hand, it was shown that low-frequency Raman investigations make possible to detect, and identify crystalline features in the early stages of crystallization (Denicourt et al., 2003; Hédoux et al., 2009), and to discriminate the emergence of crystalline features in disordered states from structural changes in the local order of amorphous states (polyamorphism) (Hédoux et al., 2001; Hédoux

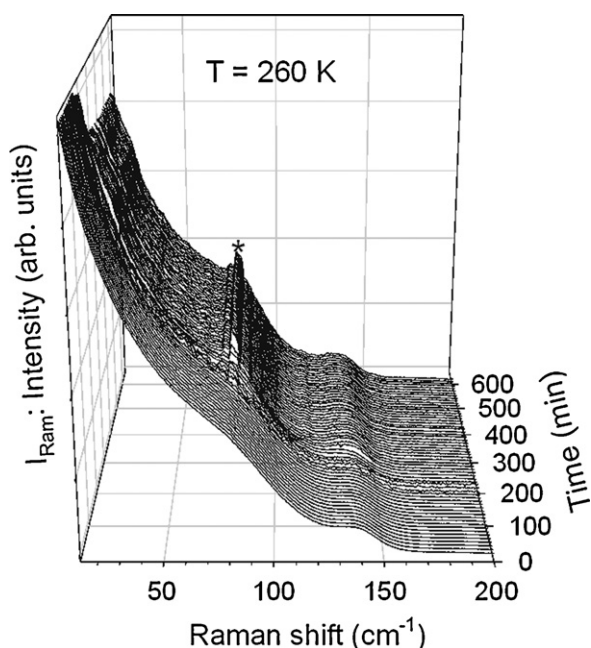


**Fig. 2.** Time dependence of the Raman intensity during the isothermal transformation of the under-cooled liquid at 260 K in set (i) of experiments. The star localizes the laser line observed after about 200 min.

et al., 2004, 2006). Consequently, the combined Raman investigations in the low- and high-frequency ranges can be considered as an indirect structural probe, well suited for the analysis of disordered systems (Hédoux et al., 2011b).

### 3. Results

In the first set of experiments (i), the new polymorphic variety of ibuprofen (phase II) was formed by imposing rigorously the thermal history to the sample described in the previous X-ray investigations (Derollez et al., 2010; Dudognon et al., 2008) and in the previous section. To analyze the isothermal transformation of the super-cooled liquid toward phase II at 260 K, the time dependence of the low-frequency Raman intensity ( $I_{\text{Ram}}(\nu)$ ) is plotted by step of 10 min in Fig. 2. The main features observed during the isothermal transformation correspond to a decrease of the QES intensity and the emergence of a hump around  $80 \text{ cm}^{-1}$ , after about 200 min of annealing at 260 K. After about 350 min no additional transformation of the low-frequency spectrum was observed. This time of transformation is consistent with the previous X-ray investigations (Derollez et al., 2010; Dudognon et al., 2008). It is worth noting that a laser line, localized by the star in Fig. 2, was observed after about 200 min of annealing. It is usually a sign of crystallization, because (micro)crystallites reflect intense light beams in any direction. Moreover, after 600 min of annealing, no remaining liquid was observed in the Lindemann glass capillary. It is therefore considered that the spectrum obtained after 600 min of annealing at 260 K is that of phase II. Intriguingly, no spectral feature in the low-frequency range can be considered as a phonon peak, as it can be expected for an ordered crystalline phase. The sample was directly cooled down to 100 K, and the low-frequency Raman spectrum is analyzed upon heating from 100 K up to 300 K by steps of 20 K. The low-frequency Raman intensity is converted into reduced intensity  $I_r(\nu) = I_{\text{Ram}}(\nu) / [(n(\nu) + 1) \cdot \nu]$ , where  $n(\nu)$  is the Bose factor. Reduced intensity is then free of band shape distortion due to thermal population effects and can be compared in Fig. 3 between 100 and 300 K. The spectrum of phase II is compared to that of phase I at 100 K in Fig. 3. This figure shows that the broad and intense low-frequency

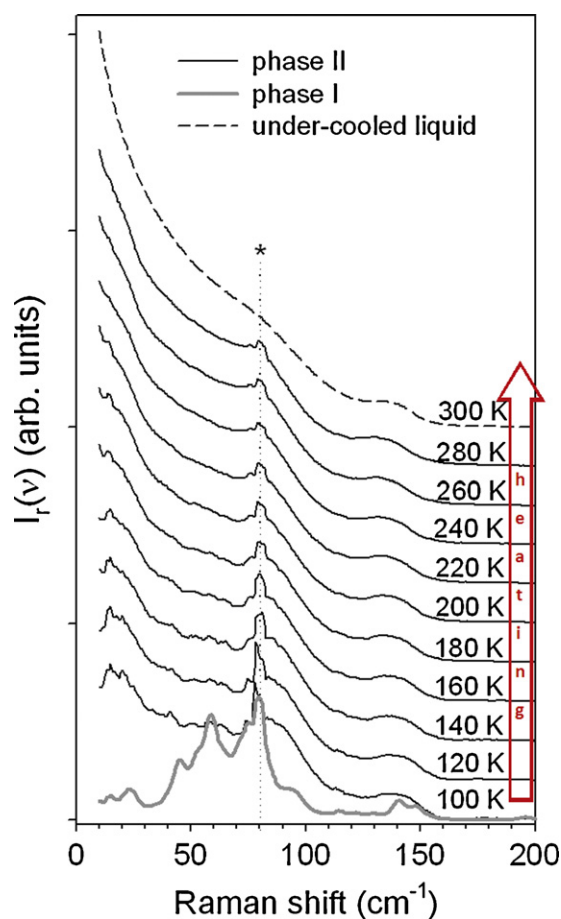


**Fig. 3.** Temperature dependence of the reduced intensity of phase II in set (i) of experiments. Spectra were taken during heating from 100 K up to 300 K. The star localizes the laser line.

contribution ( $\nu < 50 \text{ cm}^{-1}$ ) observed after isothermal transformation at 260 K, is structured in two bands at 100 K, corresponding to two phonon peaks of phase I. At 100 K, the Raman spectrum of phase II appears more structured than that obtained after isothermal transformation at 260 K. This structure, which mimics the envelope of the spectrum of phase I, disappears upon heating. Above 280 K, phase II melts, and the spectrum obtained at 300 K corresponds to that of the under-cooled liquid, in agreement with calorimetric investigations (Dudognon et al., 2008).

To obtain a better quality of Raman spectra, investigations were carried out on greater volume of powder loaded in a spherical pyrex cell, in a second set of experiments (ii). The as-received sample was heated (above  $T_m = 349 \text{ K}$ , Dudognon et al., 2008) at 360 K, rapidly quenched in the glassy state (about  $40^\circ$  below  $T_g$ ) at 190 K, and heated in the undercooled state at 260 K for isothermal annealing. As proceed in set (i), the low-frequency Raman intensity is firstly converted into reduced intensity, and then can be compared in Fig. 4a, at different temperatures in the liquid, under-cooled liquid and glassy states. Spectra were normalized by the integrated intensity in the  $80\text{--}200 \text{ cm}^{-1}$  range, from the consideration that only quasi-harmonic external motions give a contribution to the Raman spectrum in this region. In this representation, the Raman spectrum is dominated by the QES intensity in the very low-frequency range ( $< 100 \text{ cm}^{-1}$ ) (Hédoux et al., 2006, 2011b, 2009). It is clearly observed that the reduced intensity of these three states are superimposed above  $80 \text{ cm}^{-1}$ , while below this frequency the spectra are easily distinguishable. The distinction between these spectra of amorphous states in the very low-frequency range ( $5\text{--}80 \text{ cm}^{-1}$ )

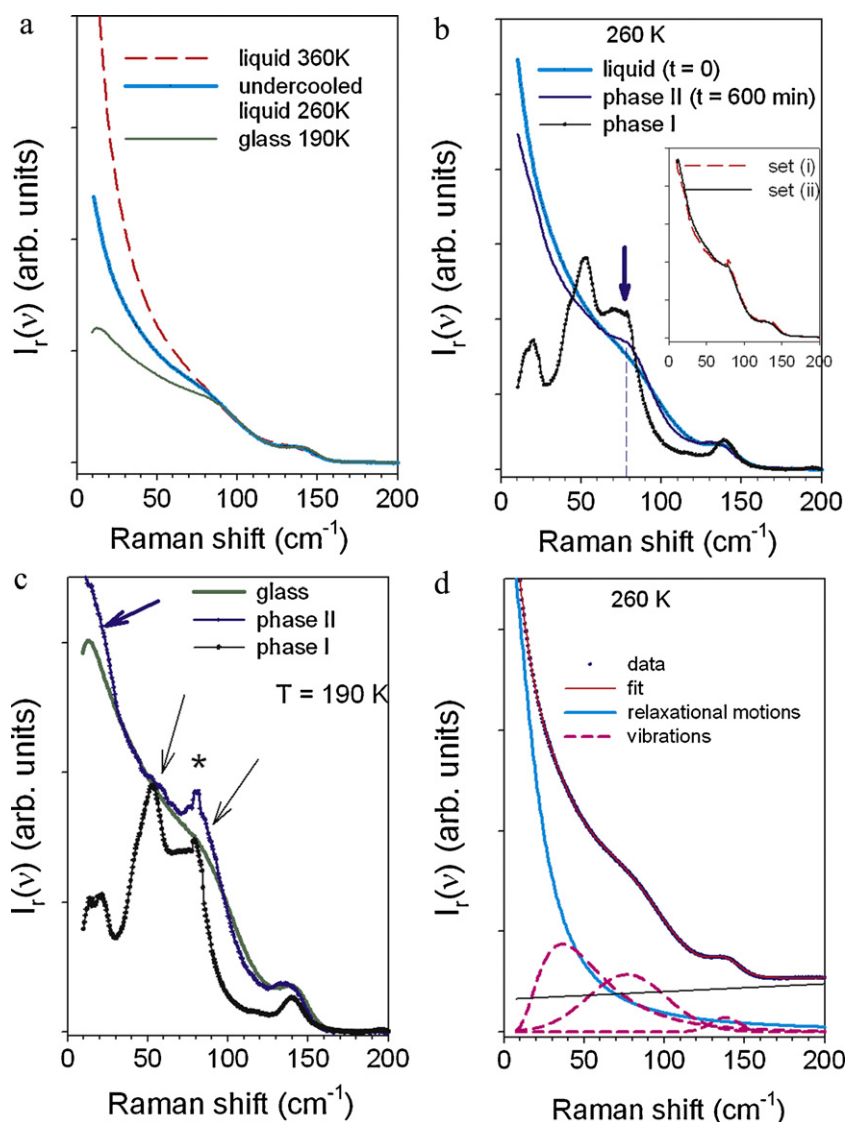


**Fig. 4.** Representation of the reduced intensity in the 5–200  $\text{cm}^{-1}$  region; all spectra are normalized by the integrated intensity in the 80–200  $\text{cm}^{-1}$ . (a) In the liquid state at  $T=360\text{ K}$ , in the undercooled liquid state at  $T=260\text{ K}$ , and in the glassy state at  $T=190\text{ K}$ , (b) at  $T=260\text{ K}$ , in the undercooled liquid at the beginning of the isothermal transformation ( $t=0$ ), in the crystalline metastable phase II at the end of the transformation ( $t=600\text{ min}$ ), and in the stable crystalline state (phase I); the arrow indicates a crystalline signature of phase I in the spectrum of phase II. The inset shows the comparison between spectra taken after 600 min of annealing at 260 K taken in the two sets of experiments. (c) At  $T=190\text{ K}$ , in the glassy state and in crystalline phases I and II; the star localizes a laser line. (d) At  $T=260\text{ K}$ , in the under-cooled liquid state, to describe the fitting procedure required to transform the reduced intensity into Raman susceptibility; blue points correspond to experimental data, the thin red line to the fit of the Raman band shape, the thick full line to the relaxational component (Lorentzian shape), and dashed lines to vibrational components.

is induced by the increase of the QES intensity inherent to the strong temperature dependence of the anharmonic semi-external motions ( $\beta$ -fast relaxations) above  $T_g \approx 228\text{ K}$ .

The time dependence of the low-frequency Raman spectrum was analyzed during the isothermal transformation at 260 K by recording spectra with an acquisition time of 120 s, every 3 min. The reduced intensity is plotted in Fig. 4b for  $t=0$  (undercooled liquid), and  $t=600\text{ min}$  (phase II), and compared with the spectrum of phase I. The spectrum obtained at  $t=600\text{ min}$  can be firstly identified as that of phase II, by comparing this spectrum with that obtained in set (i) of experiments in the inset of Fig. 4b. Spectrum of phase II can be distinguished from that of the under-cooled liquid ( $t=0$ ), from a decrease of the QES intensity and the emergence of a hump around 80  $\text{cm}^{-1}$  (see arrow of Fig. 4b), during the isothermal transformation, in agreement with set (i) of experiments. The observation of a significant contribution of the QES intensity to the spectrum of phase II, not existing in phase I, indicates the existence of semi-external motions in the crystalline phase II. The emerging

intensity around 80  $\text{cm}^{-1}$ , i.e. around a Raman band of phase I can be interpreted as the emergence of a crystalline signature of phase I.

The phase II was cooled down to 190 K to compare its reduced intensity to those of the glassy state and phase I in Fig. 4c. The spectrum of the phase II can be identified from that of the glassy state by a stronger QES component below 30  $\text{cm}^{-1}$  (see blue arrow), reflecting semi-external motions in phase II at 190 K not detected in the glassy state. Additionally, a subtle hump around 50  $\text{cm}^{-1}$  and the enhancement of the intensity near 80  $\text{cm}^{-1}$ , are observed around frequencies of Raman bands of phase I, and are probably related to crystalline features of phase I.

The determination of the spectrum corresponding to the collective harmonic vibrations, containing structural information, requires the subtraction of the QES contribution from the reduced intensity. The QES component ( $I_q(\nu)$ ) was determined by a fitting procedure of the reduced intensity as shown in Fig. 4d. It is generally well described by a Lorentzian shape, and the contribution of harmonic collective vibrations in the low-frequency range is described

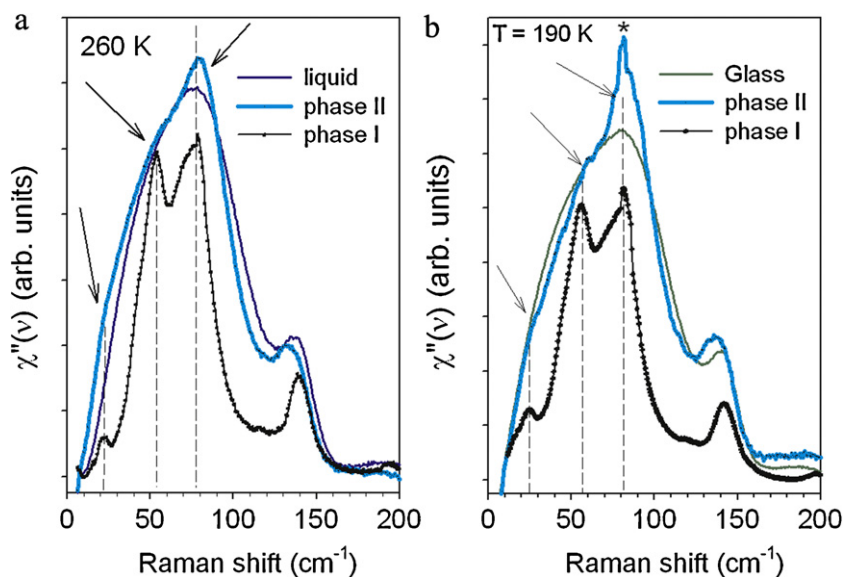


**Fig. 5.** Representation of the low-frequency (5–200  $\text{cm}^{-1}$ ) Raman susceptibility in the under-cooled (or glassy) state and crystalline phases I and II; the arrows localize the crystalline signatures of phase I detected in the spectrum of phase II. (a) At  $T=260\text{ K}$ , the spectra recorded at the beginning of the isothermal transformation ( $t=0$ ), at the end of the transformation ( $t=600\text{ min}$ , phase II), are compared to that of the stable crystalline state (phase I). (b) At  $T=190\text{ K}$ , the spectrum of glassy ibuprofen is compared to those of crystalline phases I and II.

by a lognormal function (Hédoux et al., 2001; Malinovski et al., 1991). Fig. 4d shows the overlapping of the very fast relaxational motions and low-frequency vibrations, typically on a picosecond timescale, reflecting vibrations of molecules restricted in a volume defined by the nearest molecular neighboring, the so-called cage effect in the liquid state. The reduced intensity was then converted into Raman susceptibility according to the relation (Shuker and Gammon, 1970):

$$\chi''(\nu) = I_r(\nu) \cdot \nu.$$

The Raman susceptibility is related to the vibrational density of states ( $G(\nu)$ , VDOS) by the relation:  $\chi''(\nu) = (C(\nu)/\nu)G(\nu)$ , where  $C(\nu)$  is the light-vibration coupling coefficient. This coefficient has usually a linear frequency dependence in the spectral region of the boson peak (Achibat et al., 1993; Hédoux et al., 2001). Consequently, the Raman susceptibility can be considered to be representative of the VDOS in the low-frequency range.

The Raman  $\chi''(\nu)$ -spectra of the under-cooled liquid and crystalline phases I and II are plotted in Fig. 5a. The spectrum of phase I is composed of three phonon peaks located around 20, 50 and  $80\text{ cm}^{-1}$ . Note that the Raman band observed around  $150\text{ cm}^{-1}$  in crystalline and amorphous states corresponds to an internal mode related to C–C–C deformation (Vueba et al., 2008), detected at relatively low-frequency because of the conformational flexibility of ibuprofen. The lower frequency of this band in phase II indicates higher conformational flexibility of ibuprofen in phase II than in phase I, which can lead to small conformational changes. The band-shape of the low-frequency Raman susceptibility in phase II is typical of disordered molecular systems (Affouard et al., 2001; Denicourt et al., 2003; Hédoux et al., 2011a,b; Hédoux et al., 2001, 1998; Rolland and Sauvajol, 1986) with no detection of phonon peak and the spectrum clearly appears as the envelope of the phonons of phase I. The spectrum of the phase II differs from that of the under-cooled liquid by the emergence of crystal like features of phase I, i.e. two shoulders around 20 and  $50\text{ cm}^{-1}$  and a pronounced hump around  $80\text{ cm}^{-1}$  (see arrows in Fig. 5a). Phase II appears as an intermediate state between the under-cooled liquid and the stable crystal. The Raman susceptibilities of the glassy state and crystalline phases I and II are compared at 190 K in Fig. 5b. The

spectra of the glassy state and phase II are roughly superimposed, except in the region ( $\sim 80\text{ cm}^{-1}$ ) of an intense phonon of phase I. Despite the existence of subtle shoulders in the spectrum of phase II, around 20 and  $50\text{ cm}^{-1}$ , the similar description of the VDOS spectrum of glassy ibuprofen and the  $\chi''(\nu)$ -spectrum of phase II, clearly reflects the existence of a significant disorder in phase II and a similar local molecular arrangement in glassy ibuprofen and phase II. The close structural description of the glassy state and the phase II is probably in relation to the monotropic character of the metastable phase II, only obtained after deep quench below  $T_g$  (Dudognon et al., 2008). The crystalline features of phase I, clearly observed in the Raman susceptibility of phase II, can be interpreted as the signatures of the development of the underlying long-range order of phase I, as observed in deeply under-cooled disordered systems (Denicourt et al., 2003) according to the empirical Ostwald's rule of stages (Ostwald, 1897). Indeed, from Ostwald's experience far from equilibrium states do not directly transform into the stable state but prefer to reach intermediate stages.

The Raman spectrum in the  $600\text{--}1800\text{ cm}^{-1}$  region corresponds to the fingerprint region of a molecular drug, since it is composed of intra-molecular vibrations distinctive of the atomic bonds, the molecular conformations and the close molecular neighboring. This spectral region is plotted for the glassy state and the crystalline phases at the same temperature (190 K) in Fig. 6. It is clearly observed that the spectrum of the phase II resembles that of the glassy state, reflecting a similar local order in these two states. It is worth noting that the weak Raman band detected at  $1640\text{ cm}^{-1}$  in the glassy state and the phase II, assigned to C=O stretching vibrations (Jubert et al., 2006; Rossi et al., 2009), shifts to a frequency higher than  $1650\text{ cm}^{-1}$  in phase I. Larger frequency downshifts of this band were previously observed on complexation (Rossi et al., 2009) and from the gas phase to the liquid phase (Jubert et al., 2006), and have been interpreted as resulting from the breaking of hydrogen bonds. In this context the localization of the C=O stretching band at  $1640\text{ cm}^{-1}$  probably reflects similar molecular associations in the glassy state and the phase II, which should be slightly different from the dimer association in phase I. An opposite frequency shift is observed on the Raman band assigned to vibrations of aryl ring C=C bonds (Jubert et al., 2006; Rossi et al., 2009), detected at  $1613\text{ cm}^{-1}$  in the glassy state and in phase II,

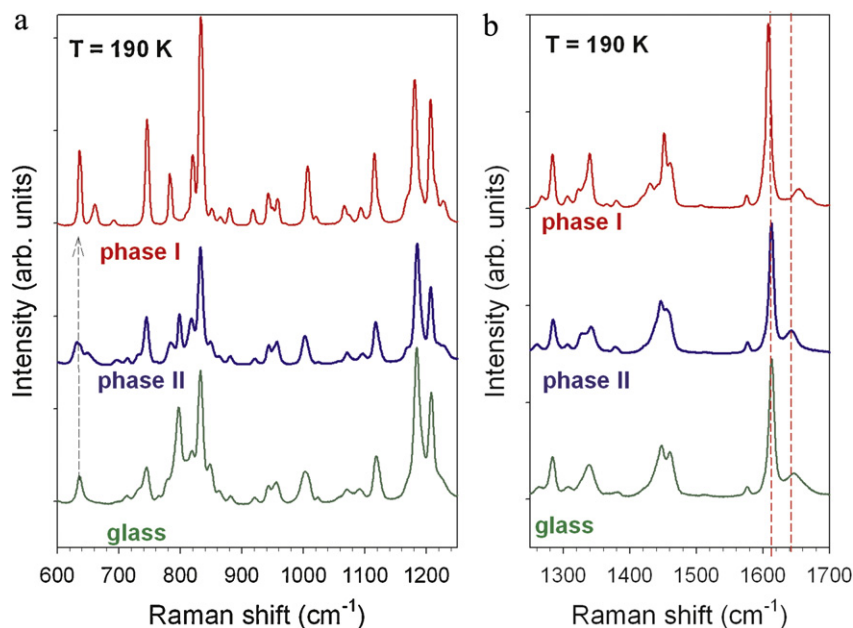


**Fig. 6.** Raman spectrum of Ibuprofen in the fingerprint region. (a) Between 600 and 1250  $\text{cm}^{-1}$ ; the arrow indicates a spectral region which appears as distinctive of each state glassy state, metastable phase II, and stable phase I and (b) between 1250 and 1750  $\text{cm}^{-1}$ ; dashed lines are guides for the eyes to point out the frequency shifts of Raman bands in the stable phase I, with respect the spectra of the glassy state and metastable phase II.

and at 1608  $\text{cm}^{-1}$  in phase I. This observation is also in agreement with previous Raman investigations (Rossi et al., 2009), suggesting different molecular associations in phase I and other phases. The spectrum of phase II differs from that of the glassy state around 635  $\text{cm}^{-1}$  and 1340  $\text{cm}^{-1}$ , respectively corresponding to the in-plane C=C ring deformation (Jubert et al., 2006; Vueba et al., 2008) and C-H bending (Jubert et al., 2006; Vueba et al., 2008), splitting into two components in phase II. However, these components appear as very broad Raman bands and become very sharper in phase I. Consequently, having regard to the single analysis of the fingerprint region for the three states (Fig. 6), phase II can be interpreted as a very disordered state, similar to the solid amorphous state.

#### 4. Discussion

Both sets of experiments (i) and (ii) provide similar low-frequency Raman spectra of phase II, with no apparent phonon peak at 260 K. Upon cooling down to 100 K, the QES contribution decreases with a structuring of the spectrum, resembling more and more to the envelope of the phonon peaks of phase I. This indicates that phase II could be described as disordered phase I, obviously less disordered at low temperature.

The isothermal transformation of the under-cooled liquid into the metastable phase II is mainly characterized by a decreased of the QES component in the 5–70  $\text{cm}^{-1}$  range and by the emergence of a hump around 80  $\text{cm}^{-1}$  corresponding to crystalline features of the stable phase. The time dependence of the QES component can be used to analyze the kinetics law associated to the isothermal transformation of the under-cooled liquid into the metastable state (phase II). The reduced intensity was integrated between 10 and 70  $\text{cm}^{-1}$ , and a degree of transformation was determined from the relation:  $\rho(t) = \left( \int_{10}^{70 \text{ cm}^{-1}} I_r(t) - I_r(t=0) \right) / \left( \int_{10}^{70 \text{ cm}^{-1}} I_r(t_{\text{end}}) - I_r(t=0) \right)$ , where  $t_{\text{end}}$  is the time of complete transformation. The time dependence of the degree of transformation is plotted in Fig. 7. This temporal evolution has a clear sigmoidal shape, distinctive of a first-order transformation and indicating the complete transformation of the

under-cooled liquid into phase II. This shape is usually associated with a nucleation and growth process. If the consideration that  $\rho(t)$  represents a volume of transformed matter is adopted, experimental data can be tentatively fitted using an Avrami-like function ( $\rho(t) = (1 - \exp(-(t/t_0)^n))$ ), where  $t_0$  is the time of half transformation and the exponent  $n$  is representative of the nucleation process and the dimensionality of the growth. Good agreement between the fitting curve and experimental data is obtained for  $t_0 = 259 \text{ min}$  ( $\pm 2$ ) and  $n = 4.3$  ( $\pm 0.2$ ). The value of the exponent suggests a dimensionality of the growth process very close to 3.

Both conversions of the low-frequency Raman intensity into reduced intensity ( $I_r(\nu)$ ) and Raman susceptibility ( $\chi''(\nu)$ ) undoubtedly reveal a strong disorder in the metastable phase II. The analysis of the reduced intensity, clearly points out the presence of semi-external motions giving an important contribution to the Raman spectrum below 70  $\text{cm}^{-1}$ , and probably corresponding to large amplitude rotations of a small group of atoms in a crystalline

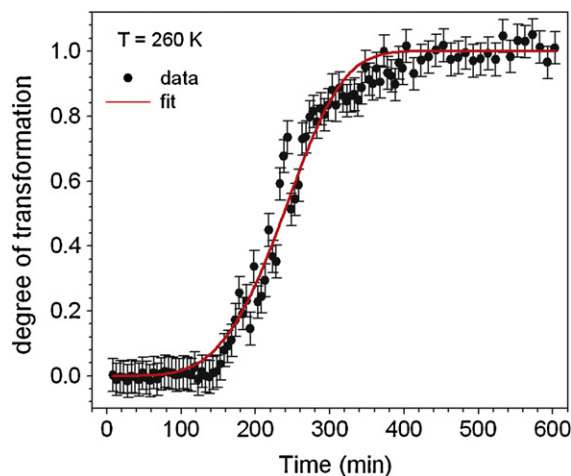


**Fig. 7.** Representation of the time dependence of the degree of the isothermal transformation  $\rho(t)$  at 260 K. Full circles correspond to experimental data and the line represents the fitting curve using an Avrami-like function.

state. This QES contribution persists at lower temperatures (190 K), as shown in Fig. 4c through an additional intensity below  $30\text{ cm}^{-1}$  in the  $I(r)$ -spectrum of phase II compared to that of the glassy state, where large molecular reorientations are considered as frozen.

The Raman susceptibility of phase II, in Fig. 5a, appears as the envelope of the broadened phonon peaks of the stable phase I. Such a band-shape for the low-frequency spectrum mimics a VDOS spectrum, as usually observed in solid amorphous states, resulting from an inhomogeneous broadening of the  $\chi''(\nu)$ -spectrum of phase II. This suggests that phase II could be described from a long-range order of dimer chains similar to that in phase I, and the consideration of static disorder responsible for the amorphous-like band-shape of the low-frequency spectrum of phase II. It is worth noting from Fig. 5a and b that the  $150\text{ cm}^{-1}$  band is detected at lower frequencies in phase II compared with amorphous (under-cooled liquid and glassy) states and phase I, indicating higher conformational flexibility of ibuprofen in phase II. Fig. 2 shows that the  $150\text{ cm}^{-1}$  band remains broadened at 100 K in phase II, while in phase I the band splits into two components. This broadened band at very low temperature can be considered as the signature of a distribution of slightly different molecular conformations in phase II.

The analysis of the  $600\text{--}1800\text{ cm}^{-1}$  region indicates that the local order in phase II is very similar to that of the glassy state, indicating the existence of disordered molecular environments in the crystalline phase II, very similar to the local organization in the glassy state. The frequency shifts observed between phases I and II for Raman bands located at  $1613$  and  $1640\text{ cm}^{-1}$  are connected to molecular associations via hydrogen bonding. Given the existence of different molecular associations determined by molecular dynamics calculations in the liquid state (Bras et al., 2008), the coexistence of different molecular associations could be the origin of the disorder in phase II.

Additional experiments have been performed in both sets (i) and (ii), with different temperatures of quenching, isothermal transformation (between 260 and 280 K), and different cooling rates. The confrontation of the different experiments reveals that obtaining phase II mainly depends on two coupled parameters; the depth of quenching and the cooling rate from the liquid toward the glassy state. Fast cooling rate (shifting the sample from a hot air stream to a cold nitrogen flux) can be associated with relatively shallow quenching ( $\sim 190\text{ K}$ , i.e. about 40 K below  $T_g$ , in set (ii)), while deep quenching (143 K) can be associated with lower cooling rate (6 K/min in set (i)) to observe the isothermal transformation of the under-cooled liquid toward phase II in the 260–280 K temperature range. In these conditions, cracks are clearly and systematically observed in the glass. Increasing the temperature of annealing between 260 and 280 K, mainly induces a drastic decrease of the time of isothermal transformation, but has no significant influence on the band shape of the spectrum of phase II. This shows that phase II can be formed reproducibly and the systematic observation of cracks prior to the isothermal transformation of the under-cooled liquid toward phase II suggests that the nucleation of this phase is probably heterogeneous and assisted by the formation of cracks in the glassy state.

## 5. Conclusions

Both low- and high-frequency Raman investigations converge into the description of phase II as disordered. The absence of phonon peaks in the low-frequency spectrum contrasts but is not inconsistent with the observation of Bragg peaks in the diffraction pattern of the metastable state, as previously reported in highly disordered plastic crystals (Denicourt et al., 2003; Hédoux et al., 2011a). Indeed, X-ray diffraction leads to the determination of the

average molecular organization and positional disorder on molecular periodic sites is therefore hardly detectable. This suggests the existence of a disordered distribution of slightly different molecular conformation and corresponding to different kinds of dimers and located at positions determined by Derollez et al. (2010), which could be the origin of a static disorder. In summary, molecular disorder is probably related to rotations of small groups of atoms (QES contribution) and to the coexistence of different molecular associations. Both kinds of disorder – dynamic and static – contribute to give the amorphous-like band-shape of the Raman susceptibility. The present investigations and the monotropic character of phase II, only obtained upon heating from a deeply under-cooled ( $T_g - 40\text{ K}$ ) state, suggest that phase II could be considered as a transient metastable state in the devitrification process toward the stable phase I, or a reproducible stage in the gradual ordering process from a far from equilibrium state toward the stable phase, in agreement with Ostwald's rule of stages (Oswald, 1897).

## Acknowledgments

Financial support to Fundação para a Ciência e Tecnologia (FCT, Portugal) through the project PTDC/CTM/098979/2008 and the Pessoa partnership Hubert Curien is acknowledged.

## References

- Achibat, T., Boukenter, A., Duval, E., 1993. Correlation effects on Raman scattering from low-energy vibrational modes in glasses II. Experimental results. *J. Chem. Phys.* 99, 2046–2051.
- Adams, S.S., Bresloff, P., Manson, C.G., 1976. Pharmacological differences between the optical isomers of ibuprofen: evidence for metabolic inversion of ibuprofen. *J. Pharm. Pharmacol.* 28, 256–257.
- Affouard, F., Hédoux, A., Guinet, Y., Denicourt, T., Descamps, M., 2001. Indication for a change of dynamics in plastic crystal chloroadamantane: Raman scattering experiment and molecular dynamics simulation. *J. Phys.: Condens. Matter.* 13, 355011–355014.
- Bras, A.R., Noronha, J.P., Antunes, M.M., Cardoso, M.M., Schonhals, A., Affouard, F., Dionisio, M., Correia, N.T., 2008. Molecular motions in amorphous ibuprofen as studied by broadband dielectric spectroscopy. *J. Phys. Chem. B* 112, 11087–11099.
- Connell, J.F., 1974. 2-(4-Isobutylphenyl) propionic acid, C13H18O2 ibuprofen or prufen. *Cryst. Struct. Commun.* 3, 73–75.
- Denicourt, T., Hédoux, A., Guinet, Y., Willart, J.F., Descamps, M., 2003. Raman scattering investigations of the stable and metastable phases of cyanoadamantane glassy crystal. *J. Phys. Chem. B* 107, 8629–8636.
- Derollez, P., Dudogon, E., Affouard, F., Danede, F., Correia, N.T., Descamps, M., 2010. Ab initio structure determination of phase II of racemic ibuprofen by X-ray powder diffraction. *Acta Crystallogr. B* 66, 76–80.
- Dudogon, E., Danede, F., Descamps, M., Correia, N.T., 2008. Evidence for a new crystalline phase of racemic ibuprofen. *Pharm. Res.* 25, 2853–2858.
- Hédoux, A., Decroix, A.-A., Guinet, Y., Paccou, L., Derollez, P., Descamps, M., 2011a. Low- and high-frequency Raman investigations on caffeine: polymorphism, disorder and phase transformation. *J. Phys. Chem. B* 115, 5746–5753.
- Hédoux, A., Derollez, P., Guinet, Y., Dianoux, A.J., Descamps, M., 2001. Low-frequency vibrational excitations in the amorphous and crystalline states of triphenyl phosphite: A neutron and Raman scattering investigation. *Phys. Rev. B* 63, 144202–144208.
- Hédoux, A., Guinet, Y., Derollez, P., Hernandez, O., Lefort, R., Descamps, M., 2004. A contribution to the understanding of the polymorphism situation in triphenyl phosphite. *Phys. Chem. Chem. Phys.* 6, 3192–3199.
- Hédoux, A., Guinet, Y., Derollez, P., Hernandez, O., Paccou, L., Descamps, M., 2006. Microstructural investigations in the glacial state of triphenyl phosphite. *J. Non-Cryst. Solids* 352, 4994–5000.
- Hédoux, A., Guinet, Y., Descamps, M., 1998. Raman signature of polymorphism in triphenyl phosphite. *Phys. Rev. B* 58, 31–34.
- Hédoux, A., Guinet, Y., Descamps, M., 2011b. The contribution of Raman spectroscopy to the analysis of transformations in pharmaceutical compounds. *Int. J. Pharm.* 417, 17–31.
- Hédoux, A., Paccou, L., Guinet, Y., Willart, J.-F., Descamps, M., 2009. Using the low-frequency Raman spectroscopy to analyze the crystallization of amorphous indomethacin. *Eur. J. Pharm. Sci.* 38, 156–164.
- Johari, G.P., Kim, S., Shanker, R.M., 2007. Dielectric relaxation and crystallization of ultraviscous melt and glassy states of aspirin, ibuprofen, progesterone and quinidine. *J. Pharm. Sci.* 96, 1159–1175.
- Jubert, A., Legarto, M.-L., Massa, N., Tevez, L., Okulik, N., 2006. Vibrational and theoretical studies of non-steroidal anti-inflammatory drugs Ibuprofen, Naproxen and Tolmetin acids. *J. Mol. Struct.* 783, 34–51.

- Lee, T., Kuo, S., Chen, Y.H., 2006. Solubility, polymorphism, crystallinity, and crystal habit of acetamophen and ibuprofen. *Pharm. Technol.* 30, 72–92.
- Malinowski, V.K., Novikov, V.N., Sokolov, A.P., 1991. Log-normal spectrum of low-energy vibrational excitations in glasses. *Phys. Lett. A* 153, 63–66.
- Nada, A.H., Al-Saidan, S.M., Mueller, B.W., 2005. Crystal modification for improving physical and chemical properties of ibuprofen. *Pharm. Technol.* 29, 90–101.
- Oswald, W., 1897. Studien über die Bildung und Umwandlung fester Körper. *Z. Phys. Chem.* 22, 289–330.
- Rasenack, N., Muller, B.B.W., 2002a. Crystal habit and tableting behavior. *Int. J. Pharm.* 244, 45–57.
- Rasenack, N., Muller, B.B.W., 2002b. Properties of ibuprofen crystallized under various conditions: a comparative study. *Drug. Dev. Ind. Pharm.* 28, 1077–1089.
- Rolland, J.-P., Sauvajol, J.-L., 1986. *J. Phys. C* 19, 3475–3480.
- Rossi, B., Verrocchio, P., Viliani, G., Mancini, I., Guella, G., Rigo, E., Scarduelli, G., Mariotto, G., 2009. Ibuprofen–cyclodextrin inclusion complexes investigated by Raman scattering and numerical simulation. *J. Raman Spectr.* 40, 453–460.
- Shankland, N., Wilson, C.C., Florence, A.J., Cox, P.J., 1997. Refinement of ibuprofen at 100 K by single-crystal pulsed neutron diffraction. *Acta Crystallogr. C* 53, 951–954.
- Shuker, R., Gammon, R., 1970. Raman-scattering selection-rule breaking and the density of states in amorphous materials. *Phys. Rev. Lett.* 25, 222–225.
- Vueba, M.L., Pina, M.E., Batista De Carvalho, L.A.E., 2008. Conformational stability of ibuprofen: assessed by DFT calculations and optical vibrational spectroscopy. *J. Pharm. Sci.* 97, 845–859.